Kinetic modelling of [^{11}C]PBR28 for 18kDa Translocator Protein PET data: a validation study of vascular modelling in the brain using XBD173 and tissue analysis

SUPPLEMENTARY MATERIAL - FIGURE 1

[^{11}C]PBR28 brain PET compartmental modelling. A) The standard 2-tissue compartmental model (2TCM) model is composed by two exchangeable tissue compartments, one describing the nondisplaceable component (C_{nd}) and one describing the specific binding (C_s). K_1 and k_2 are the rate constants for transport from plasma (C_p) to tissue and back, respectively. k_3 and k_4 are the rate constants from the nondisplaceable compartment to the specific one, respectively. B) To account for the TSPO endothelial binding, the 2TCM-1K model includes also a vascular component (C_{vasc}), with K_b rate constant from plasma to the vascular compartment. The model is approximation of the 2TCM-2K (panel C), which explicitly represents the tracer binding to TSPO in endothelial cells as reversible but does not guarantee parameter estimation (see *Study of a priori identifiability of 2TCM-2K model*).

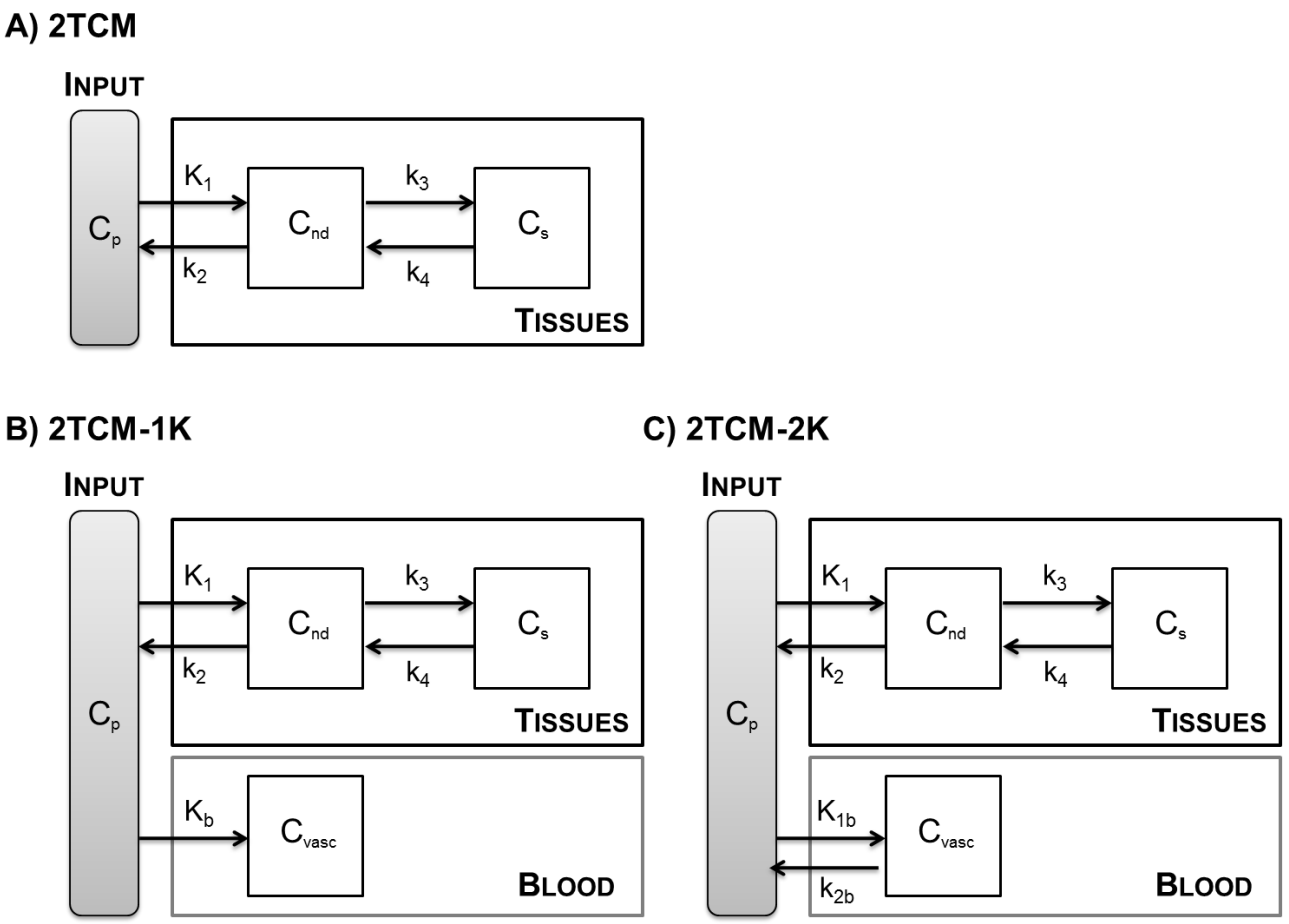

Study of a priori identifiability of 2TCM-2K model

The proposed 2TCM-2K model defined in Supplementary Figure 1C can be represented by the following system of first order differential equations:

$$\begin{aligned} \dot{C}_1(t) &= K_1 C_p(t) - (k_2 + k_3) C_1(t) + k_4 C_2(t) \\ \dot{C}_2(t) &= k_3 C_1(t) - k_4 C_2(t) \\ \dot{C}_3(t) &= K_{1b} C_p(t) - k_{2b} C_3(t) \end{aligned} \quad with \quad \begin{aligned} C_1(0) &= 0 \\ C_2(0) &= 0 \\ C_3(0) &= 0 \end{aligned} \qquad \text{(A1)}$$

The total amount of radioactivity measured by PET, $C_{measured}(t)$, is the summation of different contributes:

$$C_{measured}(t) = (1 - V_b)[C_1(t) + C_2(t)] + V_b C_b(t) + V_b C_3(t) \qquad \text{(A2)}$$

where $C_1(t) + C_2(t)$ represents the activity of the tracer in the target tissues, C_b the activity in the whole blood, C_3 the tracer in the blood vessel endothelium, and V_b the fraction of volume occupied by blood over the tissue within the considered field of view. To evaluate the *a priori* uniquely identifiability of 2TCM-2K we exploit transfer function approach (***Bertoldo et al, "Kinetic modeling of [(18)F]FDG in skeletal muscle by PET: a four-compartment five-rate-constant model", Am J Physiol Endocrinol Metab, 2001***) . By taking the Laplace transforms of Eq. A1 and rearranging it, one has

$$\begin{aligned} sC_1(s) &= K_1 C_p(s) - (k_2 + k_3) C_1(s) + k_4 C_2(s) \\ sC_2(s) &= k_3 C_1(s) - k_4 C_2(s) \\ sC_3(s) &= K_{1b} C_p(s) - k_R C_3(s) \end{aligned} \qquad \text{(A3)}$$

Solving for C_1,C_2 and C_3

$$\begin{aligned} C_1(s) &= \frac{K_1(s + k_4)}{s^2 + s(k_2 + k_3 + k_4) + k_2 k_4} C_p(s) \\ C_2(s) &= \frac{K_1 k_3}{s^2 + s(k_2 + k_3 + k_4) + k_2 k_4} C_p(s) \\ C_3(s) &= \frac{K_{1b}}{s + k_{2b}} C_p(s) \end{aligned} \qquad \text{(A4)}$$

Thus the Laplace transform of $C_{measured}(t)$ can be written as

$$C_{measured}(s) = (1 - V_b)\left[\frac{K_1(s + k_4)}{s^2 + s(k_2 + k_3 + k_4) + k_2k_4} \cdot \left(1 + \frac{k_3}{(s + k_4)}\right)\right] C_p(s) + V_b C_b(s) + V_b \frac{K_{1b}}{s + k_{2b}} C_p(s) \quad \text{(A5)}$$

which leads to:

$$C_{measured}(s) = \frac{s^2[(1 - V_b)K_1 + V_bK_{1b}] + s[(1 - V_b)K_1(k_3 + k_4 + k_{2b}) + V_bK_{1b}(k_2 + k_3 + k_4)] + (1 - V_b)K_1(k_3k_{2b} + k_4k_{2b}) + V_bK_{1b}k_2k_4}{s^3 + s^2(k_2 + k_3 + k_4 + k_{2b}) + s(k_2k_{2b} + k_3k_{2b} + k_4k_{2b} + k_2k_4) + k_2k_4k_{2b}} C_p(s) + V_bC_b(s) \quad \text{(A6)}$$

The exhaustive summary of the model is given by

$$\begin{aligned}
\phi_1 &= (1 - V_b)K_1 + V_bK_{1b} \\
\phi_2 &= (1 - V_b)K_1(k_3 + k_4 + k_{2b}) + V_bK_{1b}(k_2 + k_3 + k_4) \\
\phi_3 &= (1 - V_b)K_1(k_3k_{2b} + k_4k_{2b}) + V_bK_{1b}k_2k_4 \\
\phi_4 &= k_2 + k_3 + k_4 + k_{2b} \\
\phi_5 &= k_2k_{2b} + k_3k_{2b} + k_4k_{2b} + k_2k_4 \\
\phi_6 &= k_2k_4k_{2b} \\
\phi_7 &= V_b
\end{aligned} \quad \text{(A7)}$$

where $\phi_1, \ldots, \phi_6$ are the known observational parameters. The 7 parameters $K_1, k_2, k_3, k_4, K_{1b}, k_{2b}$ and V_b are not *a priori* identifiable.

SUPPLEMENTARY MATERIAL - FIGURE 2

Immunostain for TSPO in the adrenal cortex (A) shows ubiquitous expression in cortical cells (C) while the medulla (M) is negative; western blot analysis shows a single 18kDa band that is the expected molecular weight of a TSPO monomer (B).

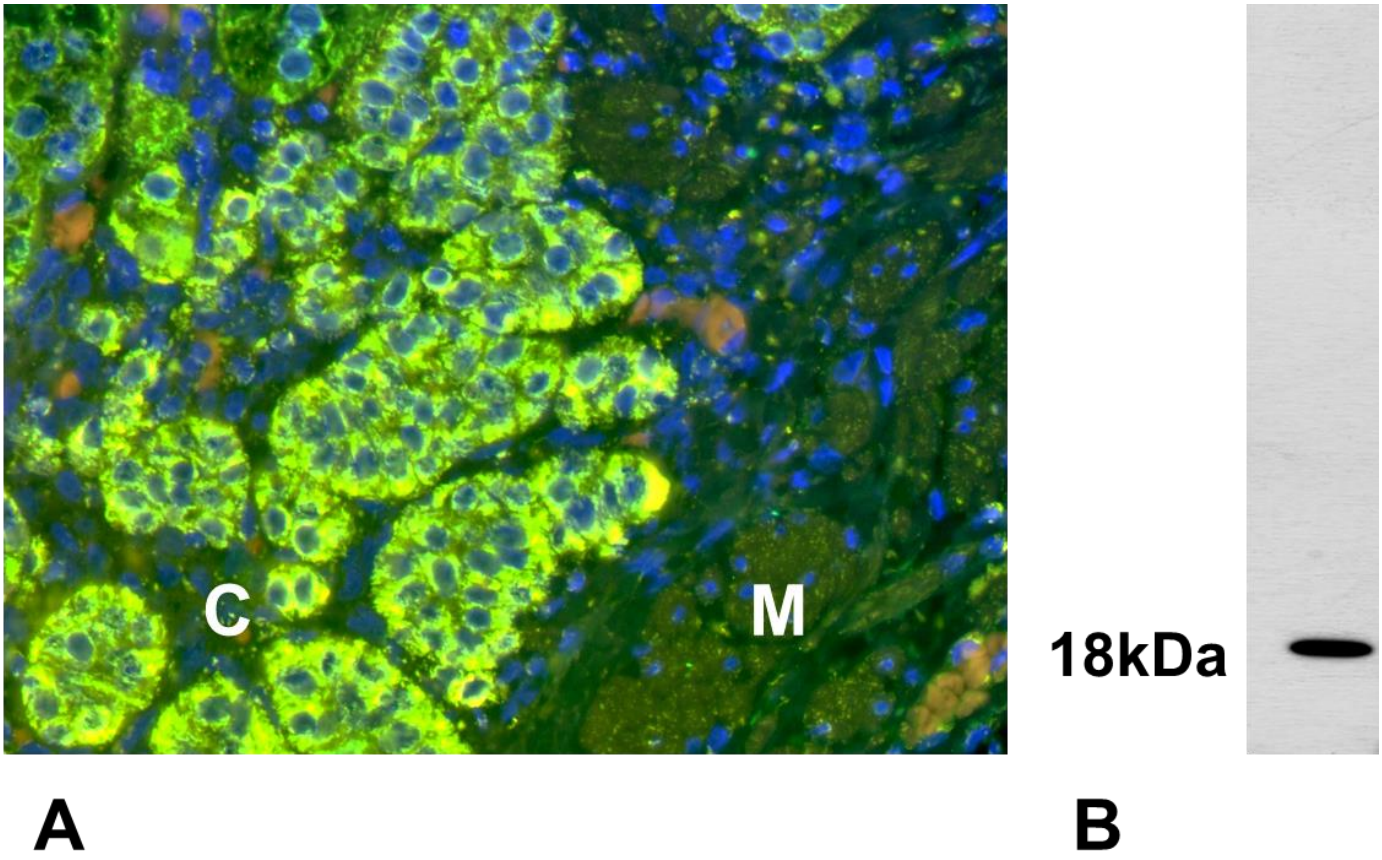

SUPPLEMENTARY MATERIAL - FIGURE 3

*[^{11}C]PBR28 brain PET tissue uptake before and after TSPO blocking***.** A) Baseline scan. B) Blockage with 90 mg XBD173. Both PET scans refer to the same representative patient with schizophrenia, quantified with SUV at minute 90 after tracer injection.

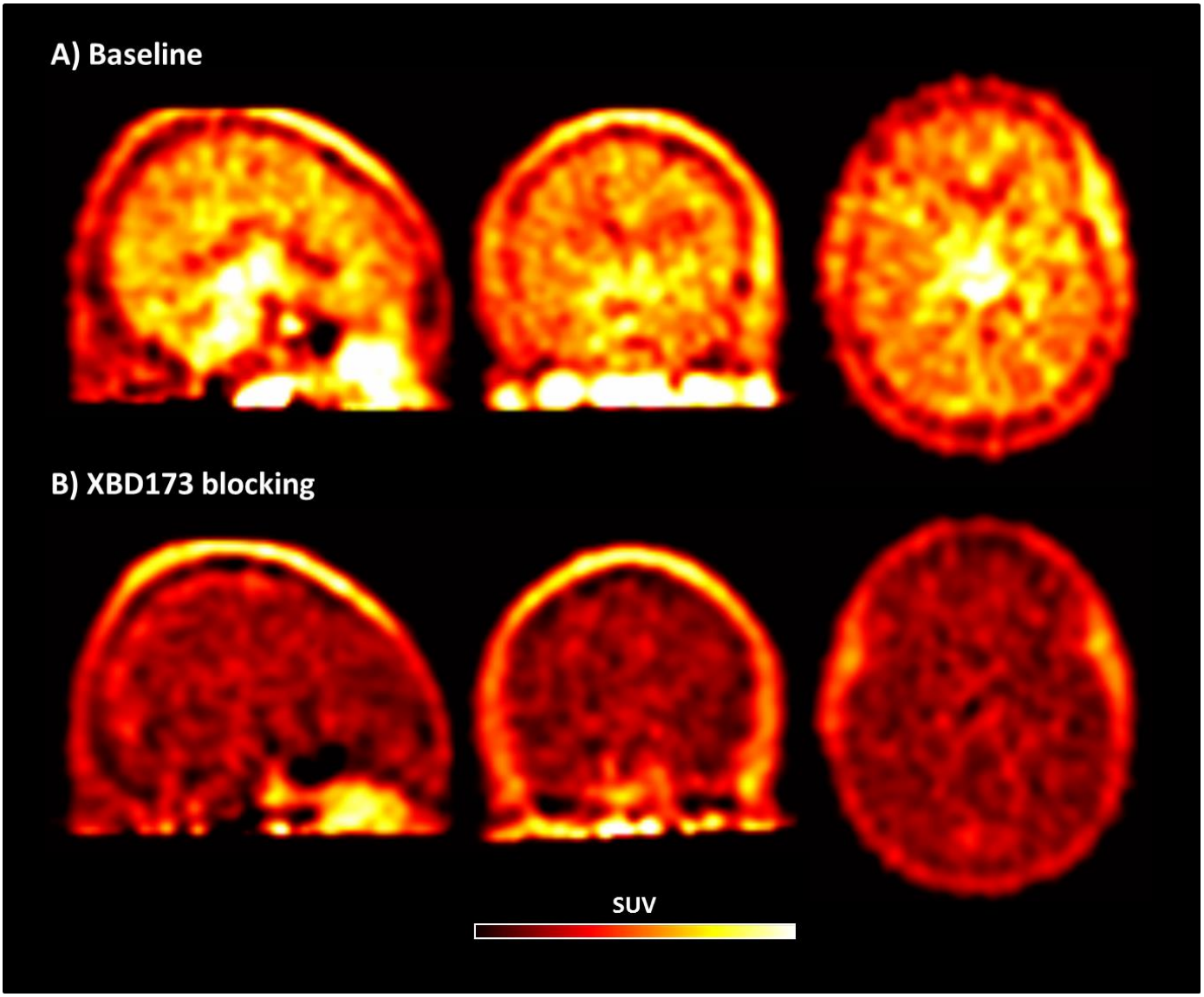

SUPPLEMENTARY MATERIAL - FIGURE 4

*Normal and abnormal [11C]PBR28 brain PET tracer kinetics***.** The figure compares the regional tissue kinetics in two subjects with normal (A) and abnormal (B) [11C]PBR28 uptake respectively. Regional TACs are shown for whole brain, grey matter (GM) and thalamus, both in baseline and after XBD173 blockage. In the first subject (normal [11C]PBR28 brain PET kinetics) there is a clear effect of XBD173 on regional TACs compared to baseline. This pattern is consistent with the other 5 participants included in the study. In the second subject (abnormal [11C]PBR28 brain PET kinetics) the effect of XBD173 is less visible, and regional TACs are more similar to those measured at baseline, both in shape and amplitude. Plasma concentrations of XBD173 were not measured, hence we cannot verify whether this subject had unusual pharmacokinetics, or whether this is within the range of experimental variability.

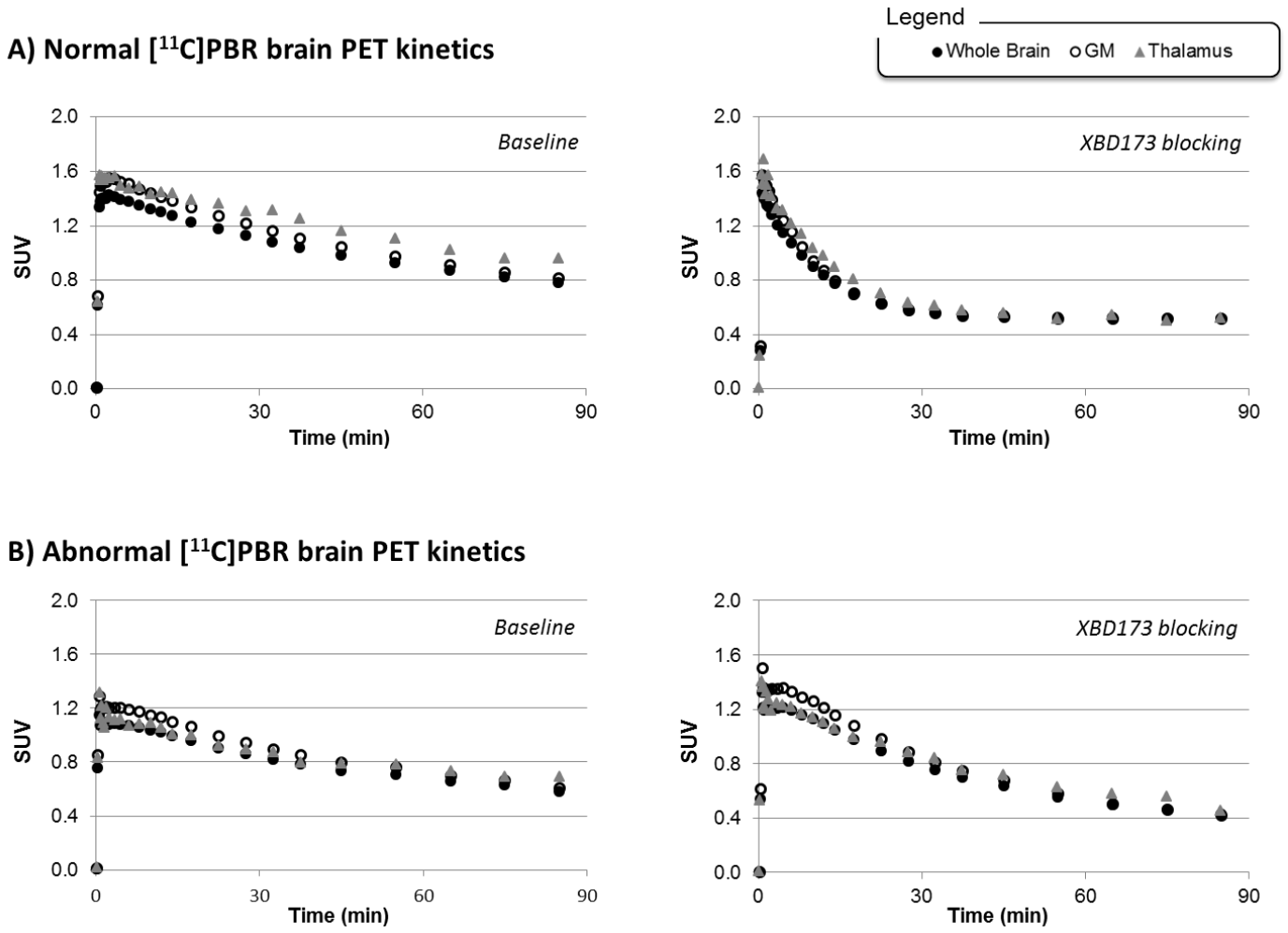

SUPPLEMENTARY MATERIAL - FIGURE 5

The figure shows the regional TSPO brain expression as derived by Allen Brain Atlas (A) and its comparison with [^{11}C]PBR28 PET changes between baseline and after XBD173 blockage (B). V_T kinetic estimate changes computed for 2TCM-1K and 2TCM (red and blue circles, respectively) and SUV calculated at 90 minutes after tracer injection (black triangles) are linear correlated with TSPO mRNA expression across brain ROIs. For each modelling approach, the predicted mRNA values are reported as function of the TSPO mRNA measures.

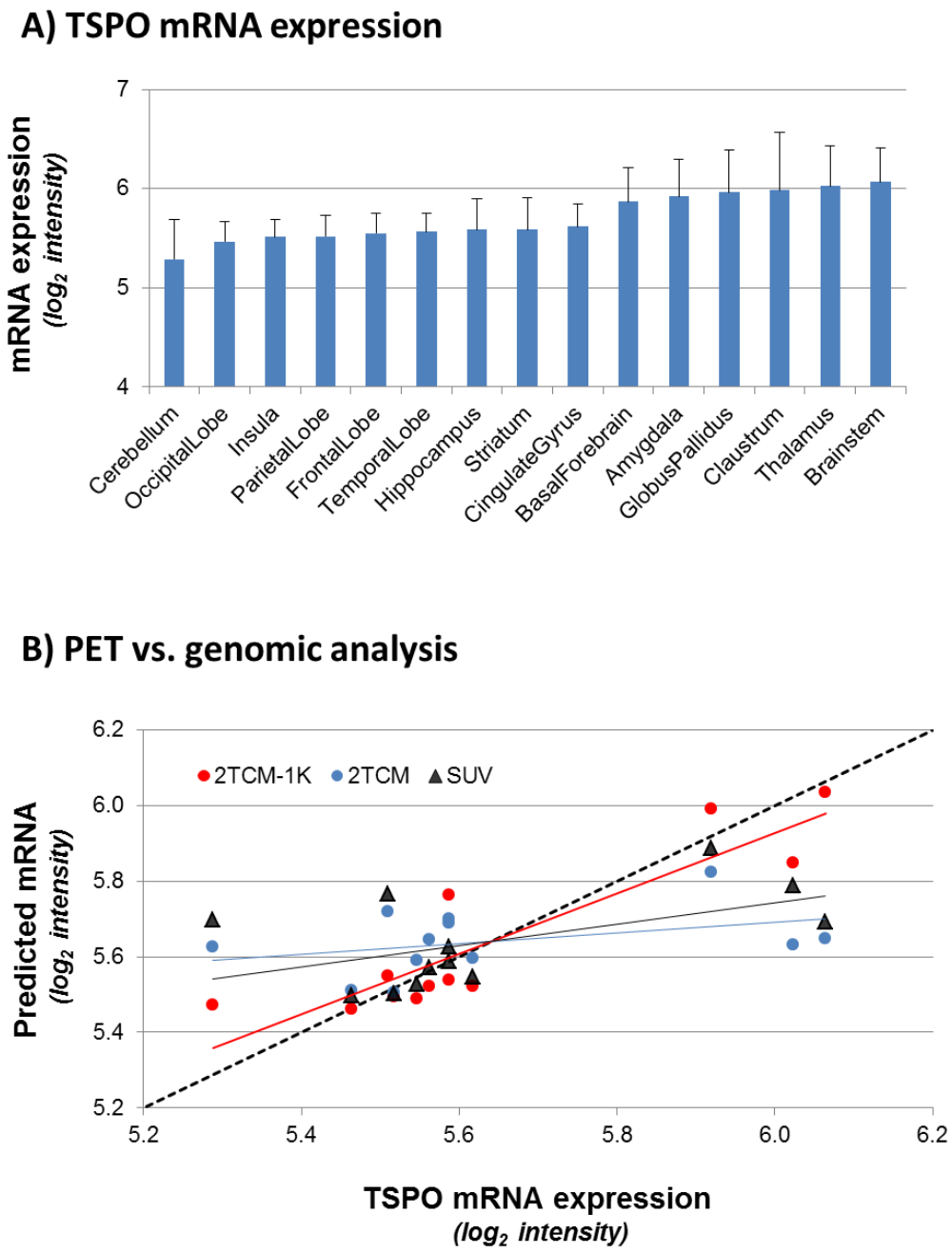

SUPPLEMENTARY MATERIAL - FIGURE 6

TSPO mRNA expression from purified representative populations of neurons, astrocytes, oligodendrocyte precursor cells, newly formed oligodendrocytes, myelinating oligodendrocytes, microglia, endothelial cells, and pericytes from mouse cerebral cortex. mRNA expression is reported in Fragments Per Kilobase of transcript per Million mapped reads (FPKM). Source: Zhang, Ye, et al. "An RNA-sequencing transcriptome and splicing database of glia, neurons, and vascular cells of the cerebral cortex." *The Journal of Neuroscience* 34.36 (2014): 11929-11947.

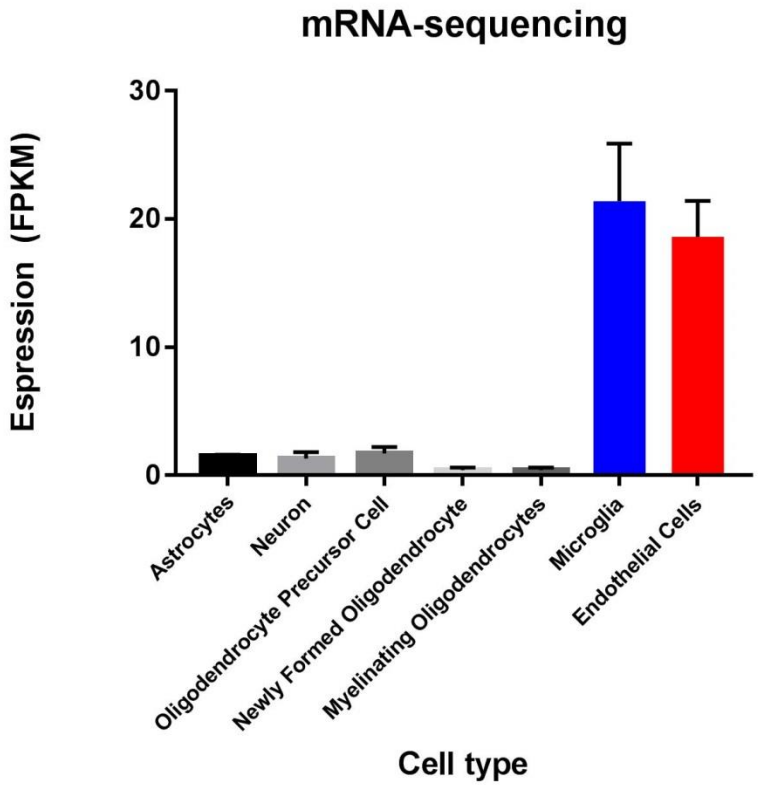

SUPPLEMENTARY MATERIAL – Table 1

AIC comparison. The table shows mean+SD estimates of AIC as obtained for the 2TCM and 2TCM-1K models respectively. Mean+SD individual regional relative differences (($AIC_{2TCM-1K}$ - AIC_{2TCM})/ abs(AIC_{2TCM})) are also reported.

	2TCM			2TCM-1K			Individual Rel. Diff.		
ROIs	**Mean**	**±**	**SD**	**Mean**	**±**	**SD**	**Mean**	**±**	**SD**
Whole brain	-43.6	±	16.7	-69.1	±	36.7	-67%	±	76%
White Matter	-46.5	±	8.1	-66.4	±	20.5	-44%	±	46%
Grey Matter	-43.1	±	19.3	-66.8	±	40.0	-74%	±	81%
Occipital Lobe	-34.1	±	18.2	-46.7	±	23.9	-54%	±	83%
Temporal Lobe	-39.9	±	21.7	-52.9	±	32.4	-68%	±	92%
Frontal Lobe	-49.7	±	17.4	-73.3	±	40.0	-53%	±	71%
Parietal Lobe	-43.9	±	18.2	-69.3	±	34.5	-72%	±	83%
Amygdala	-4.9	±	7.2	-5.1	±	13.6	-6%	±	128%
Hippocampus	-13.0	±	13.9	-19.3	±	17.3	-29%	±	83%
Thalamus	-15.3	±	9.2	-32.5	±	19.5	-60%	±	115%
Striatum	-24.9	±	16.3	-30.6	±	13.9	-19%	±	41%
Cerebellum	-30.6	±	24.5	-41.5	±	31.9	-34%	±	80%

SUPPLEMENTARY MATERIAL – Table 2

[^{11}C]PBR brain PET kinetic analysis with 2TCM-1K

	V_T (mL/cm^3)		K_1/k_2 (mL/cm^3)		k_3/k_4 (unitless)	
ROIs	***Baseline***	***Blocking***	***Baseline***	***Blocking***	***Baseline***	***Blocking***
Whole brain	2.31 ± 0.63	0.70 ± 0.26	0.60 ± 0.15	0.46 ± 0.18	3.18 ± 0.56	0.56 ± 0.11
White Matter	1.34 ± 0.38	0.62 ± 0.10	0.39 ± 0.09	0.29 ± 0.11	2.58 ± 0.47	1.32 ± 0.47
Grey Matter	2.64 ± 0.71	0.76 ± 0.34	0.67 ± 0.17	0.52 ± 0.22	3.28 ± 0.58	0.47 ± 0.11
Occipital Lobe	2.56 ± 0.73	0.70 ± 0.31	0.64 ± 0.18	0.49 ± 0.21	3.38 ± 0.61	0.45 ± 0.10
Temporal Lobe	2.43 ± 0.75	0.73 ± 0.29	0.58 ± 0.14	0.47 ± 0.20	3.53 ± 0.74	0.57 ± 0.11
Frontal Lobe	2.49 ± 0.65	0.73 ± 0.30	0.64 ± 0.15	0.49 ± 0.21	3.22 ± 0.72	0.50 ± 0.09
Parietal Lobe	2.42 ± 0.67	0.71 ± 0.31	0.65 ± 0.17	0.49 ± 0.21	3.07 ± 0.55	0.47 ± 0.11
Amygdala	2.49 ± 1.55	1.14 ± 0.22	0.55 ± 0.18	0.57 ± 0.15	3.61 ± 1.33	0.99 ± 0.53
Hippocampus	2.59 ± 1.07	1.04 ± 0.35	0.64 ± 0.21	0.49 ± 0.19	3.36 ± 0.78	1.24 ± 0.64
Thalamus	2.45 ± 0.78	0.90 ± 0.29	0.59 ± 0.17	0.50 ± 0.22	3.30 ± 0.42	0.82 ± 0.27
Striatum	2.62 ± 1.03	0.74 ± 0.18	0.73 ± 0.27	0.45 ± 0.14	2.93 ± 0.41	0.72 ± 0.27
Cerebellum	2.71 ± 0.65	0.78 ± 0.34	0.67 ± 0.18	0.51 ± 0.23	3.38 ± 0.69	0.50 ± 0.11

SUPPLEMENTARY MATERIAL – Table 3

[^{11}C]PBR brain PET kinetic analysis with 2TCM

	V_T (mL/cm^3)		K_1/k_2 (mL/cm^3)		k_3/k_4 (unitless)	
ROIs	***Baseline***	***Blocking***	***Baseline***	***Blocking***	***Baseline***	***Blocking***
Whole brain	4.72 ± 1.18	2.16 ± 1.05	1.09 ± 0.27	0.56 ± 0.13	3.68 ± 1.10	2.99 ± 1.66
White Matter	4.30 ± 0.95	1.97 ± 0.58	0.75 ± 0.16	0.44 ± 0.14	5.01 ± 1.02	3.72 ± 1.05
Grey Matter	4.95 ± 1.26	2.45 ± 1.62	1.19 ± 0.30	0.60 ± 0.13	3.52 ± 1.09	3.30 ± 2.40
Occipital Lobe	4.76 ± 1.26	2.91 ± 2.36	1.24 ± 0.35	0.57 ± 0.13	3.21 ± 1.05	2.89 ± 1.89
Temporal Lobe	4.82 ± 1.16	2.06 ± 0.85	1.05 ± 0.24	0.59 ± 0.13	3.99 ± 1.22	2.62 ± 1.34
Frontal Lobe	4.81 ± 1.21	2.43 ± 1.57	1.12 ± 0.26	0.57 ± 0.12	3.62 ± 1.13	3.42 ± 2.34
Parietal Lobe	4.64 ± 1.18	2.91 ± 2.65	1.17 ± 0.27	0.56 ± 0.12	3.28 ± 1.01	2.59 ± 1.19
Amygdala	6.67 ± 2.09	1.62 ± 0.53	1.19 ± 0.42	0.61 ± 0.22	5.14 ± 1.81	1.77 ± 0.75
Hippocampus	5.25 ± 1.23	1.88 ± 0.51	1.13 ± 0.27	0.59 ± 0.15	3.91 ± 1.07	2.14 ± 0.59
Thalamus	5.70 ± 1.28	1.79 ± 0.45	1.09 ± 0.18	0.59 ± 0.11	4.47 ± 1.00	4.55 ± 5.58
Striatum	4.83 ± 1.01	1.86 ± 0.60	1.19 ± 0.20	0.59 ± 0.20	3.16 ± 0.77	2.38 ± 1.04
Cerebellum	4.87 ± 1.25	2.27 ± 1.44	1.17 ± 0.35	0.58 ± 0.12	3.61 ± 1.27	3.02 ± 2.12

SUPPLEMENTARY MATERIAL – Table 4

Endothelial binding estimates. The table shows the vascular binding estimates (K_b, 1/min) at baseline and after TSPO blockade. Mean±SD, across 7 patients with schizophrenia are reported for several ROIs, together with percentage mean relative differences (m.r.d.) between conditions.

ROIs	***Baseline***	***Blocking***	***m.r.d.***
Whole brain	0.32 ± 0.14	0.14 ± 0.06	-51% ± 21%
White Matter	0.52 ± 0.17	0.23 ± 0.06	-55% ± 9%
Grey Matter	0.29 ± 0.13	0.13 ± 0.06	-50% ± 26%
Occipital Lobe	0.30 ± 0.16	0.14 ± 0.07	-49% ± 26%
Temporal Lobe	0.26 ± 0.10	0.13 ± 0.07	-48% ± 28%
Frontal Lobe	0.31 ± 0.14	0.14 ± 0.06	-48% ± 24%
Parietal Lobe	0.30 ± 0.13	0.14 ± 0.06	-49% ± 18%
Amygdala	0.25 ± 0.11	0.11 ± 0.09	-65% ± 30%
Hippocampus	0.26 ± 0.15	0.11 ± 0.08	-52% ± 34%
Thalamus	0.38 ± 0.17	0.14 ± 0.07	-60% ± 15%
Striatum	0.42 ± 0.22	0.14 ± 0.07	-53% ± 25%
Cerebellum	0.33 ± 0.21	0.14 ± 0.07	-49% ± 25%

SUPPLEMENTARY MATERIAL – Table 5

TSPO volume analysis for four regions of interest. All measurements are taken in a 500 μm3 volume.

Frontal Lobe – Grey matter

Regions	CD31	TSPO	Ratio CD31:TSPO
ROI 1	181.81	60.56	3:1
ROI 2	305.90	122.72	2.5:1
ROI 3	199.49	61.59	3.2:1
Mean	229.07	81.62	2.8:1

Frontal Lobe – White matter

Regions	CD31	TSPO	Ratio CD31:TSPO
ROI 1	224.45	52.51	4.3:1
ROI 2	254.32	125.66	2:1
ROI 3	266.88	49.37	5.4:1
Mean	248.55	75.85	3.3:1

Cerebellum – Grey matter

Regions	CD31	TSPO	Ratio CD31:TSPO
ROI 1	323.29	62.07	5.2:1
ROI 2	359.66	63.98	5.6:1
ROI 3	375.19	107.93	3.5:1
Mean	352.71	77.99	4.5:1

Cerebellum – White matter

Regions	CD31	TSPO	Ratio CD31:TSPO
ROI 1	442.59	140.16	3:1
ROI 2	541.27	159.92	3:1
ROI 3	596.72	175.61	3.4:1
Mean	526.86	158.52	3.3:1

SUPPLEMENTARY MATERIAL – TSPO 3D reconstruction in normal human brain

The stained slides were scanned at the University of Manchester (UoM) Bioimaging Facility under the supervision of trained imaging technicians competent in the use of a 3D Histech Pannoramic 250 Flash slide scanner (3DHISTECH Ltd. Budapest, HUNGARY). Once scanned, slides were stored on the UoM imaging database and were accessed from dedicated terminals using the Caseviewer software package (3DHISTECH Ltd). Caseviewer was used to set magnification and localise viewpoint to a specific and constant region of interest. Slides were converted manually from a .JPEG format into .TIFF files for upload into the ImageJ scientific image analysis and alteration tool. Regions of interest were converted manually from their native format ".mrcs" into .TIFF files using the bioformat plugin in ImageJ to facilitate further aligning and stacking.

Orientation of the slide stacks took place using the bioformat plugin in ImageJ with slides uploaded to the tool in a .TIFF format using the Bioimager plugin. Prior to stacking, RGB images were converted in ImageJ and were treated with colour deconvolution plugin (https://imagej.nih.gov/ij/) using the 'Fastred Fastblue DAB' setting in order to minimise interference from blue counterstaining. Generated images were further orientated and aligned automatically in ImageJ using the StackReg plugin with orientation a rigid approach. The mapping of coordinates takes the form $x = \{ \{\cos\theta, -\sin\theta\}, \{\sin\theta, \cos\theta\} \} \cdot \mathbf{u} + \Delta\mathbf{u}$. Around conserved areas of fluorescence as deemed by the plugin (P. Thévenaz, U et al., IEEE Transactions on Image Processing, vol. 7, no. 1, pp. 27-41, January 1998). Whilst this approach was deemed the most appropriate, automatic orientation was not always accurate for this studies purpose and thus the TrackEM2 plugin was used to manually highlight regions of vascular similarity and finetune automatic orientation by hand.

It is worth noting that in order for stained regions to be visualised three dimensionally in the Imaris Biplane software (Bitplane AG Zurich, Switzerland), the stacks were altered from a red, green, blue channel format into greyscale following orientation. Imaris processed images as simply 'stained' and 'unstained' sections with background reduced at analyser's discretion. Stacks were uploaded in .TIFF, greyscale format and bitplane's Imaris 3D viewer was used to analyse the orientated slide stacks and produce 3D images of baseline TSPO and CD31 distribution in healthy brain tissue.

An example of stacking and 3D reconstruction of vessels and vascular TSPO expression is reported below; eighty consecutive sections of frontal lobe including arachnoid (A), grey matter (GM) and white matter (WM) are first immunostained for CD31 (sections 1, 3, 5, …, 79) and TSPO

(sections 2, 4, 6, …, 80). The sections are scanned and stacked using the Image J programme. This figure shows three dimensional reconstructions of a selected region of interested (ROI) in the cortex. Arbitrary colours are given to represent the vascular network in red and TSPO expression in green.